

PAPER • OPEN ACCESS

Levitation, oscillations, and wave propagation in a stratified fluid

To cite this article: Marina Carpineti *et al* 2021 *Eur. J. Phys.* **42** 055011

View the [article online](#) for updates and enhancements.



IOP | ebooksTM

Bringing together innovative digital publishing with leading authors from the global scientific community.

Start exploring the collection—download the first chapter of every title for free.

Levitation, oscillations, and wave propagation in a stratified fluid

Marina Carpineti^{1,*} , Fabrizio Croccolo²  and Alberto Vailati¹ 

¹ Dipartimento di Fisica Aldo Pontremoli, Università degli Studi di Milano, I-20133 Milano, Italy

² Université de Pau et des Pays de l'Adour, E2S UPPA, CNRS, TotalEnergies, LFCR UMR5150, Anglet, France

E-mail: marina.carpinetti@unimi.it

Received 28 January 2021, revised 11 June 2021

Accepted for publication 29 June 2021

Published 20 July 2021



CrossMark

Abstract

We present an engaging levitation experiment that students can perform at home or in a simple laboratory using everyday objects. A cork, modified to be slightly denser than water, is placed in a jug containing tap water and coarse kitchen salt delivered at the bottom without stirring. The salt gradually diffuses and determines a stable density stratification of water, the bottom layers being denser than the top ones. During the dissolution of salt, the cork slowly rises at an increasing height, where at any instant its density is balanced by that of the surrounding water. If the cork is gently pushed off its temporary equilibrium position, it experiences a restoring force and starts to oscillate. Students can perform many different measurements of the phenomena involved and tackle non-trivial physical issues related to the behaviour of a macroscopic body immersed in a stratified fluid. Despite its simplicity, this experiment allows to introduce various theoretical concepts of relevance for the physics of the atmosphere and stars and offers students the opportunity of getting acquainted with a simple system that can serve as a model to understand complex phenomena such as oscillations at the Brunt–Väisälä frequency and the propagation of internal gravity waves in a stratified medium.

Keywords: education, levitation, hydrodynamics, stratified fluids

 Supplementary material for this article is available [online](#)

*Author to whom any correspondence should be addressed.



Original content from this work may be used under the terms of the [Creative Commons Attribution 4.0 licence](#). Any further distribution of this work must maintain attribution to the author(s) and the title of the work, journal citation and DOI.

(Some figures may appear in colour only in the online journal)

1. Introduction

The levitation of macroscopic objects has fascinated humankind for a very long time. Its history is intertwined with the research performed by several Nobel laureates, because beyond its mystical aspects levitation can be profitably used both as a tool in fundamental research and in technological applications [1, 2]. Beyond its historical role in science, the investigation of levitation is still full of puzzling results, such as the apparent reversal of the gravity acceleration recently reported for a solid body at the surface of a levitating liquid [3, 4].

The fascination determined by levitation comes from the fact that we rarely experience it, as objects close to the surface of the Earth do not float freely into the air, due to the strong gravitational attraction and the small buoyancy force exerted by air onto solid bodies. When the gravitational force is not balanced, the object is in free fall, and in the frame of reference of the falling object, the acceleration of gravity is not felt. This determines weightlessness levitation conditions that can be employed profitably to perform experiments in the absence of gravity on platforms such as drop towers, parabolic flights, and artificial satellites like the International Space Station [5]. On Earth, the gravitational force acting on a body can be also balanced by the buoyancy force acting onto it when the body is immersed in a fluid medium. When the density of the body equals that of the surrounding fluid, the weight of the body is exactly balanced by the buoyancy force and the body is in equilibrium inside the fluid neither rising nor sinking, in a condition similar to levitation. However, the phenomenon of levitation does not involve simply the balance of forces, as occurs in buoyancy phenomena, but the mechanical stability of the levitating body [6]. The particularity of a levitation phenomenon is that restoring forces drive back the body when it is moved away from its equilibrium position.

A levitation condition can occur in a stable stratified medium, where the density decreases as a function of height. A body can therefore be in equilibrium only at a certain height where its density is exactly matched and a displacement in a direction parallel to the density gradient determines a restoring force that brings back the object to the layer of fluid with the same density. This force gives rise to damped harmonic oscillations that occur at a frequency, known as Brunt–Väisälä frequency [7], which is determined by the local density gradient present in the stratified fluid. The oscillations gradually damp both through viscous dissipation and through the emission of transverse internal gravity waves propagating in the plane perpendicular to the direction of oscillation. Examples of natural systems where a density stratification occurs include giant planets and stars [8], where the mass is large enough to determine the confinement of a fluid phase. A typical example is represented by the atmosphere of a planet, where the stratification of a gaseous phase is due to the variation of pressure with altitude, which determines a gradual decrease of density.

In this work, we discuss a simple experiment that can be realized by students using kitchenware to investigate levitation, oscillations at the Brunt–Väisälä frequency, and internal gravity waves in a stratified medium. The experiment makes use of a modified cork that sinks into water but suddenly starts levitating when a large enough saline gradient is generated by pouring coarse salt inside water. Its simplicity makes this demonstration suitable for students starting from elementary school up to undergraduate school, due to the opportunity of achieving different levels of understanding and modelling of the physical processes involved.

For undergraduate students, in particular, the experiment can be used to convey the hydrostatic principles behind the balance of the forces involved. Moreover, an external perturbation of the cork allows the investigation of the physics of oscillations in a stratified medium and the radiative transfer of the energy of oscillations determined by internal gravity waves.

The paper is organized as follows. The first paragraph reviews the experimental contexts where levitation is observed in nature, in order to give a general framework where the experiment may be inserted. In the following, we present the experiment, discuss its relevance in an educational context, and describe the experimental materials and methods. We then provide the basic theoretical concepts needed to describe the hydrostatic equilibrium of a fluid and the conditions that can give rise to either buoyancy or levitation of a body embedded in it. We discuss the case of the oscillations of a body in equilibrium in a stratified fluid and the internal gravity waves originated by the dissipation of energy during the oscillations. Finally, we describe, analyse and discuss the experimental results.

2. Levitation in science

Although it hardly occurs spontaneously in nature, levitation has been profitably used in science to perform several challenging experiments. A notable example of its usage in fundamental research is represented by the celebrated experiment by Robert Millikan for the measurement of the charge of the electron, where a negatively charged droplet of oil was levitated by using an electrostatic field [9]. Millikan was awarded the Nobel prize in physics in 1923 for this experimental demonstration of the discrete nature of the electric charge [10]. Levitation can also be achieved by using a magnetic field, as it happens for example by placing a superconducting disk above a strong magnet [1, 11, 12]. Magnetic levitation has important technological applications for the development of frictionless railways [13, 14]. A strong magnetic field can also be used for challenging applications like the levitation of a living being, as it has been done in a popular experiment by Andre Geim and Michael Berry. By using a strong magnetic field, they were able to levitate a living frog, and this result allowed them to win the Ig-Nobel prize in physics in the year 2000 [15]. Beyond the use of external fields, levitation can be also achieved by using radiation [1]. The phenomenon of acoustic levitation was studied by Rayleigh. Currently, acoustic levitation can be even achieved by amateurs at home or in the classroom, by building affordable instrumentation based on off-the-shelf components such as Tiny-Lev [16], a device that allows levitating small objects with a maximum size of 4 mm and density below 2 g cm^{-3} . The levitation of particles using light can be achieved by using optical tweezers, developed by Ashkin [17], an invention that allowed him to win the Nobel prize in physics in 2018 [18]. Optical tweezers allow the non-invasive manipulation of nanoparticles by taking advantage of a focussed laser beam that exerts a non-isotropic radiation pressure, resulting in the trapping of a particle in a potential well. The introduction of optical tweezers determined a revolution in the fields of biophysics and soft matter, where they allow the investigation of the behaviour of colloidal particles, molecular motors, and cells, to mention just a few representative applications [19, 20].

Neutral buoyancy represents a condition similar to levitation, very common in the case of animals populating the waters of the Earth. Meaningful strategies adopted by marine animals to achieve neutral buoyancy are represented by the swim bladder of teleost fish, by the squalene oil contained in large quantities into the liver of sharks, and by the large hollow chambers built by the nautilus into its shell [21]. In the case of marine animals, neutral buoyancy is achieved in a medium of nearly constant density, and this feature determines an indifferent equilibrium condition, where the weight of the animal can be balanced by buoyancy irrespectively of the position of the animal. The lack of a unique equilibrium position and of a restoring force indicates that neutral buoyancy cannot properly be considered a levitation phenomenon.

In the presence of a stable density stratification, the equilibrium condition can be well described as levitation. In particular, when the density gradient evolves in time, it is possible to observe that an object, initially at rest, suddenly starts to rise under the action of invisible

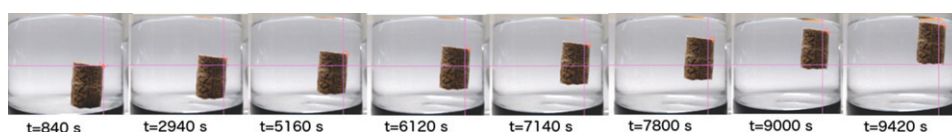


Figure 1. Shots of the cork during its rise. The marked point and the reference axis used for tracking are shown. Coordinates are fixed so that the origin coincides with the position of the tracked point at the starting time. For each figure, the time of acquisition from the beginning of the measurement is shown.

forces. At any instant, its equilibrium is at a well-defined height where it is subjected to restoring forces that make it oscillate in case it is slightly displaced. Several macroscopic systems exhibit these conditions and share the common feature that the mechanical energy associated with the local oscillation can be transferred at a distance by internal gravity waves generated by the oscillation itself. Gravity waves originate inside the bulk of a fluid in the presence of a density stratification when a displacement of a portion of the fluid is restored by gravity. This mechanism is similar to that of surface waves but occurs in the bulk of the fluid and is well described in [22], which also provides an instructing and general tutorial about waves in fluids.

Although internal gravity waves in a fluid cannot be visualized, the effect of the energy transferred by them at a distance can be appreciated from the effect that it has on macroscopic bodies embedded in the fluid. An important example is represented by the Earth's atmosphere, where mountain reliefs and thunderstorms can interact with gravity waves to give rise to complex turbulent phenomena [7]. Another notable example is represented by oceans, where the density stratification is determined by changes both in salinity and temperature. Internal gravity waves have been reported also at the mesoscale in laboratory experiments on non-equilibrium fluids, where the displacement of parcels of fluids is determined by the thermal energy $k_B T$ [23].

3. The experiment

The experiment is ideally presented to students through an inquiry based path, where the phenomenology is first demonstrated to the students by a facilitator. Students are then instructed about the details of the experiment so that they can perform it autonomously. Eventually, the students are lectured about the physical principles behind the experiment and about the methods for the analysis of results.

3.1. Inquiry-driven presentation of the experiment

Levitation is a surprising, intriguing, and counter-intuitive theme that offers the chance to discuss many physical phenomena. It is extremely difficult to observe it in practice and all the experiments involving it require a great technological effort. In this work, we describe a very simple levitation experiment, where a weighed-down cork, initially located at the bottom of a glass jug containing water, suddenly starts levitating inside the fluid and gradually rises (figure 1).

Apparently, no source of energy is involved in the process, and this leaves the students with a first scientific puzzle: (i) *where does the mechanical work needed to raise the cork come from?* Another striking aspect of this experiment is that when the levitating cork is slightly displaced vertically from its position, it undergoes damped harmonic oscillations (figure 2).

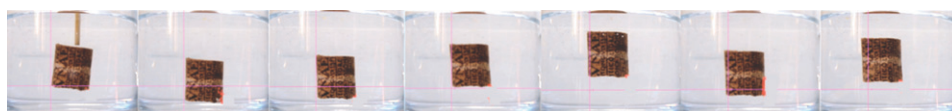


Figure 2. Shots of the cork during oscillation induced by a slight initial push. A video is included as supplemental material (video 1) (<https://stacks.iop.org/EJP/42/055011/mmedia>).



Figure 3. Two corks in a tank. After some oscillations of the right cork, also the left cork starts to move although with an oscillation amplitude much lower than the first cork. A video is included as supplemental material (video 2).

This aspect leaves the students with a second puzzling question: (ii) *what is the physical origin of the restoring force that drives the cork towards its equilibrium position during oscillations?*

When two levitating corks are hosted inside the same container, pushing one of the corks vertically determines, after a latency time, the onset of oscillations in the second cork as well (figure 3). This feature raises a third puzzling question for the students: (iii) *what is the origin of the interaction between the two corks?*

3.2. Materials and methods

For the experiment we had in mind, we needed an easy-to-find object, with a density slightly larger than water. The choice was to weigh-down the cork of a wine bottle. The cork was cut in two halves digging a hole in each of them to host a weight, for which we chose another item frequently available at home: a steel marble with a diameter of 10 mm borrowed from a toy. We soaked the sphere in vinyl glue, pasted back the two halves of the cork (see figure 4), and used ethyl cyanoacrylate glue along the junction. Finally, we cut thin slices of the cork, until it had a density slightly larger than water and was able to sink into it.

The experiment is prepared by pouring 500 ml of tap water into a cylindrical glass jug, and adding a defined amount of coarse kitchen salt without applying any stirring, so that the salt grains rapidly sediment to the bottom of the jug. We decided to use coarse rather than fine salt to avoid its partial dissolution while settling at the bottom of the jug, and therefore guarantee to start from better-defined initial conditions. However, by using fine salt, the setting up of a density gradient, and therefore the levitation process can become much faster. The experiment is started by rapidly putting the cork at the bottom before the salt has much time to dissolve. The cork, initially sitting at the bottom of the jug, is expected to start to levitate when the



Figure 4. The picture on the left shows the two halves of the cork, with the hemispherical dimples carved into them, both filled with vinyl glue and one of them hosting the metal sphere. The picture on the right shows the assembled cork. In this configuration, the cork density was still smaller than that of water and it was necessary to cut thin slices of the cork to make it slightly denser than water.

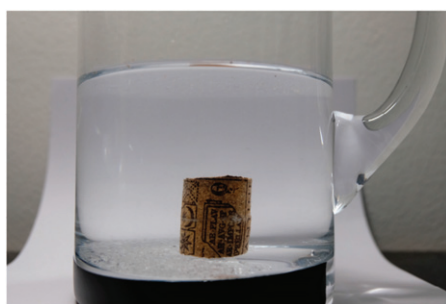


Figure 5. Picture of the starting time of a typical measurement. The cork lies at the bottom of the jug where the coarse salt has settled.

surrounding density becomes higher than its own and to move towards a height where an iso-density condition is reached. The process occurs because the salt undergoes a diffusion process that determines a density stratification in the water: the salt-rich layers of fluid at the bottom of the jug are initially denser than the salt-poor layers at the top. Diffusion determines the spread of the salt ions across water, until eventually they become uniformly distributed inside the available volume (figure 5).

Once the density of the cork is chosen, measurements can be performed with different amounts of salt that determine the behaviour of the cork. We span densities varying from 10 to 46 g l⁻¹.

In our experiment, for the smaller amounts used (typically 10–15 g l⁻¹), the cork rises after some time but eventually goes back to the bottom of the jug, because the equilibrium density (i.e. for infinite time) of the aqueous solution is smaller than that of the cork. For larger amounts of salt, the cork rises at the beginning and eventually reaches the top of the liquid, finally floating at its surface. In the latter case, the equilibrium density of the liquid is larger than that of the cork. Refining the quantity of salt dissolved in the tap water around the values obtained for the two different conditions, one can get a somewhat precise measurement of the density of the cork. We could estimate its density to be approximately 1.030 g cm⁻³, starting from

an estimation of the critical amount of salt of 40 g dissolved in 1 kg of tap water, although the cork density can slightly change from one experiment to another due to its moisture content.

The cork ascent lasts usually many hours and we recorded it using a Fujifilm XT20 camera programmed to shoot pictures at regular time intervals, typically every 5 min. The framing is chosen so as to capture the entire height of the liquid. In order to study the oscillation process, we apply a punctual acceleration to the cork and record its oscillations at 24 frames/second by using the same camera. Should this experiment be proposed to students, even a readily available smartphone could be used to make many of the measurements and this was indeed the procedure followed at the beginning. However, when available, an automated system is definitely preferable.

Both cork's rise and oscillations were characterized using the open source software 'Tracker' [24], a Java-based application that allows to track the different positions of an object in a video. To analyse the cork's ascent, the sequence of collected images has been first converted in an AVI video, using the Fiji open source software [25], and then imported into Tracker, setting the correct frame rate. Spatial calibration is done for each video by assigning to the water height the real value previously measured with a ruler (6.8 cm). To track the different positions of the cork, a mark is then placed at a recognizable point of it, such as a corner or a small detail, and the origin of the reference system is fixed on it. Due to a large number of frames to analyse, the choice of a well-identifiable and non-ambiguous point is extremely important to allow the use of the auto-tracking procedure, much faster than the manual one. At the end of the process, the different positions of the point as a function of time are obtained.

4. Theory review

In this section, we will provide the basic physical concepts needed for the understanding of the hydrostatic equilibrium of a fluid, which can give rise to the levitation of a body embedded into it and, consequently, to its oscillations when it is gently pushed off its equilibrium position, and to the generation of internal gravity waves. To achieve an understanding of the physics involved in all these processes, we will try to give an answer to the following three fundamental questions, following an approach similar to that of Enrico Fermi for the understanding of sound waves [26]:

- (a) Under which conditions a body immersed in a density layered fluid is in mechanical equilibrium?
- (b) How does a body immersed in a layered medium vibrate when subjected to a small perturbation?
- (c) How does the layered medium inside which the body is immersed transfer its vibration?

The answer to the first question will lead to the fundamental result that the layered medium determines the presence of a stable equilibrium.

The second question will be answered by solving the equation of motion determined by the forces acting on the body, and assuming that the surrounding medium is not perturbed by its presence. Answering the third question requires understanding how the energy of the oscillating body is transferred to the surrounding liquid, and this requires writing the nonlinear set of hydrodynamic equations for the layered medium. The analytical solution of this nonlinear system of equations is an impervious feat unless one linearizes them by assuming that the perturbation determined by the oscillating body is small.

4.1. Hydrostatic equilibrium, buoyancy, and levitation

Let us consider a very general configuration suitable to describe fluids such as the atmosphere and oceans: a fluid of density ρ , distributed in a layer of thickness L . A parcel of fluid of volume V is under the action of the gravity force $F = \rho Vg$, where g is the acceleration of gravity. At a height z , the weight of the column of fluid above it determines a hydrostatic pressure p inside the fluid, governed by the equation:

$$\nabla p = \rho \mathbf{g}. \quad (1)$$

In the case of an incompressible fluid like a liquid, the density is constant and the hydrostatic pressure is governed by Stevino's equation

$$p(z) = p_0 - \rho gz \quad (2)$$

which is a particular solution of equation (1), where p_0 is the pressure at the surface of the fluid $z = 0$.

A consequence of the hydrostatic pressure of equation (1) is that a body of volume V_0 completely immersed in the fluid is subjected to forces acting perpendicularly to its surface S . As the horizontal components are balanced, the body is under the action of a buoyancy force \mathbf{F}_A directed vertically, which can be obtained by integrating the hydrostatic pressure provided by equation (2) across the surface S of the body:

$$F_A = - \left| \oint_S p(z) d\mathbf{S} \right| = \int_{V_0} \frac{dp}{dz} dV = \rho g V_0, \quad (3)$$

where $d\mathbf{S}$ is an element of the surface with outgoing normal, and we have applied the divergence theorem to convert a surface integral to a volume integral.

The total force acting on the body can be obtained by adding to the buoyancy force the weight of the body $\rho_0 V_0 g$ with the proper sign:

$$F_T = (\rho - \rho_0) g V_0, \quad (4)$$

where ρ_0 is the density of the body. An immediate consequence of equation (4) is that when the density of the body is matched with that of the fluid, $F_T = 0$. A major limitation of neutral buoyancy is that it requires a very close matching between the density of the fluid and that of the body. Even a small difference between these quantities would give rise to a condition where the body is under the action of a constant acceleration, which brings it progressively farther from its initial position.

A stable equilibrium condition can be achieved by immersing the body in a stratified compressible fluid, like for example a gas stratified by the gravity force. Under this condition, the body migrates to the layer of fluid matching its density. This condition is difficult to obtain in practice because the average density of most solid bodies is much larger than that of a gas. Matching the density of the solid would require the use of a liquid, which is intrinsically not compressible and, therefore, cannot be stratified by the gravity force.

Notwithstanding that, a gravitationally stable density stratification can be obtained in a liquid under non equilibrium conditions. In fact, if the liquid is under the action of a vertical temperature gradient ∇T its thermal expansion determines a density gradient $\nabla \rho = \frac{\partial \rho}{\partial T} \nabla T$. Moreover, if the liquid is a mixture of two components, a variation of the concentration c with height determines a density gradient $\nabla \rho = \frac{\partial \rho}{\partial c} \nabla c$. In general, combining these two terms, the overall vertical density gradient is given by:

$$\nabla \rho = \rho (\alpha \nabla T + \beta \nabla c), \quad (5)$$

where α is the thermal expansion coefficient, and β is the solutal expansion coefficient.

Under the condition that the overall density gradient points downwards, the density profile is gravitationally stable, and a body of density ρ_0 such as $\rho_{\min} < \rho_0 < \rho_{\max}$ can levitate in a layer of a stratified fluid.

4.2. Oscillations in a stratified fluid

Let us now consider the case where a body of density ρ_0 and volume V_0 is immersed in a layer, with the same density, of a gravitationally stable stratified fluid. If the volume V_0 undergoes a small displacement z in the vertical direction, the density gradient can be assumed to be locally constant so that the density changes linearly with height:

$$\rho(z) = \bar{\rho} + \frac{\partial \rho}{\partial z} z. \quad (6)$$

Combining equations (1), (3) and (6), one can calculate the buoyancy force acting on volume V_0 :

$$F_B = - \oint_S p(z) d\mathbf{S} = \int_{V_0} \frac{dp}{dz} dV = \rho_0 g V_0 + \frac{\partial \rho}{\partial z} g V_0 z \quad (7)$$

and recalling equation (4) the total force acting on V_0 is:

$$F_T = \frac{\partial \rho}{\partial z} g V_0 z. \quad (8)$$

By applying the second principle of dynamics $\rho_0 V_0 \ddot{z} = F_T$, one obtains the equation of motion of a harmonic oscillator (notice that $\frac{\partial \rho}{\partial z}$ is negative):

$$\ddot{z} = \frac{g}{\rho_0} \frac{\partial \rho}{\partial z} z, \quad (9)$$

where oscillations occur at the Brunt–Väisälä frequency [7]:

$$N = \sqrt{-\frac{g}{\rho_0} \frac{\partial \rho}{\partial z}}. \quad (10)$$

Oscillations at the Brunt–Väisälä frequency also occur when a parcel of fluid is displaced vertically with respect to the surrounding fluid. This process occurs in natural systems such as the atmosphere and the oceans and in astrophysical systems such as stars. Interestingly, the same physical mechanism drives oscillations at mesoscopic length scales during a thermal diffusion process occurring in a mixture of fluids [23]. In that case, the density stratification stems from temperature and concentration gradient, thus resulting in an additional contribution related to the temperature gradient. Anyway, the equation can be written in the same form of equation (10) of the present paper if one considers the dependence from the density gradient.

4.3. Internal gravity waves

When either a portion of the fluid or a body embedded into it oscillates, its mechanical energy is gradually transferred to the surrounding fluid. Part of the energy undergoes viscous dissipation, while another part gets transferred at a distance by the layered fluid in the form of an internal gravity wave. Although internal gravity waves are qualitatively similar to the surface waves in a liquid, their density gradient is, of course, much smaller than that of surface waves and

the absence of a sharp interface makes them more difficult to detect. In the following we will describe the emission and propagation of transverse waves by a body that undergoes vertical harmonic oscillations at the Brunt–Väisälä frequency in a stratified fluid.

For a more rigorous and general treatment of internal gravity waves see Tritton [27] and Nappo [7].

We consider an incompressible inviscid fluid in the presence of a stable density stratification described by equation (6). The Eulerian hydrodynamic equations for a fluid of velocity \mathbf{u} , pressure p' and density ρ' are:

$$\nabla \cdot \mathbf{u} = 0 \quad (11)$$

$$\rho' \frac{\partial \mathbf{u}}{\partial t} + \rho' \mathbf{u} \cdot \nabla \mathbf{u} = -\nabla p' + \rho' \mathbf{g} \quad (12)$$

$$\frac{\partial \rho'}{\partial t} + \mathbf{u} \cdot \nabla \rho' = 0. \quad (13)$$

Equation (11) is the continuity equation and expresses the conservation of mass, while equation (12) is the second law of dynamics and equation (13) expresses the fact that the fluid is not compressible.

We assume that the variables for the fluid in motion with velocity \mathbf{u} can be written as a superposition of an hydrostatic contribution and a small perturbation:

$$p'(x, y, z, t) = p(z) + \delta p(x, y, z, t) \quad (14)$$

$$\rho'(x, y, z, t) = \rho(z) + \delta \rho(x, y, z, t), \quad (15)$$

where p and ρ obey the hydrostatic equations. $\nabla p = \rho \mathbf{g}$ and $\partial \rho / \partial t = 0$, respectively. By inserting equations (14) and (15) into equations (11)–(13), we obtain:

$$\nabla \cdot \mathbf{u} = 0 \quad (16)$$

$$\rho \frac{\partial \mathbf{u}}{\partial t} + \delta \rho \frac{\partial \mathbf{u}}{\partial t} + \rho \mathbf{u} \cdot \nabla \mathbf{u} + \delta \rho \mathbf{u} \cdot \nabla \mathbf{u} = -\nabla \delta p + \delta \rho \mathbf{g} \quad (17)$$

$$\frac{\partial \delta \rho}{\partial t} + \mathbf{u} \cdot \nabla \rho + \mathbf{u} \cdot \nabla \delta \rho = 0. \quad (18)$$

We now assume that the perturbations of density and pressure are small with respect to the hydrostatic quantities, $|\delta p/p| \ll 1$ and $|\delta \rho/\rho| \ll 1$, and linearize the equations in \mathbf{u} , δp , and $\delta \rho$:

$$\nabla \cdot \mathbf{u} = 0 \quad (19)$$

$$\rho \frac{\partial \mathbf{u}}{\partial t} = -\nabla \delta p + \delta \rho \mathbf{g} \quad (20)$$

$$\frac{\partial \delta \rho}{\partial t} + \mathbf{u} \cdot \nabla \rho = 0. \quad (21)$$

We look for solutions of the equations in the form of propagating harmonic waves of wave vector \mathbf{k} and frequency ω :

$$\mathbf{u} = \mathbf{U} \exp[i(\mathbf{k} \cdot \mathbf{x} - \omega t)] \quad (22)$$

$$\delta \rho = R \exp[i(\mathbf{k} \cdot \mathbf{x} - \omega t)] \quad (23)$$

$$\delta p = P \exp[i(\mathbf{k} \cdot \mathbf{x} - \omega t)]. \quad (24)$$

For simplicity, we restrict ourselves to a two-dimensional system, of coordinates x (horizontal), and z (vertical). We assume that the parcel of fluid is located in the origin of the coordinate system at time $t = 0$, and undergoes harmonic motion in the vertical direction. This implies that the amplitude \mathbf{U} of the oscillation in equation (22) must be directed in the vertical direction, that is $\mathbf{U} = (0, U)$.

By imposing that equation (22) must be a solution of the continuity equation (19) we obtain that the velocity must be perpendicular to the wave vector:

$$\mathbf{U} \cdot \mathbf{k} = 0 \Rightarrow k_z = 0. \quad (25)$$

Therefore, the velocity wave defined by equation (22) is transverse, and its wave vector is directed horizontally, $\mathbf{k} = (k, 0)$.

By imposing that equations (23) and (24) are solutions of equations (20) and (21) we get:

$$kP = 0 \Rightarrow P = 0 \quad (26)$$

$$i\omega\rho U = gR \quad (27)$$

$$i\omega R = \frac{d\rho}{dz} U. \quad (28)$$

Equation (26) implies that the pressure does not propagate and the dissipation of energy does not occur through the emission of a sound wave. Multiplication of equations (27) and (28) allows to determine the frequency of the internal gravity waves, which coincides with the Brunt–Väisälä frequency of the oscillating parcel of fluid:

$$\omega = \sqrt{-\frac{g}{\rho_0} \frac{\partial \rho}{\partial z}} = N. \quad (29)$$

Notice that, although this theoretical model confirms that the harmonic motion of a parcel of fluid in the vertical direction gives rise to transverse internal gravity waves propagating horizontally, the wave number and the velocity of the wave are not predicted by it, and in principle, there are no constraints on the values that k and the velocity can assume.

5. Results and discussion

We performed various experiments using different amounts of salt, ranging between 10 and 46 g l⁻¹. In each measurement, we tracked the cork's rise until its position was approximately at half of the water height. Then, we took movies of the oscillations in order to measure the Brunt–Väisälä frequency.

In figure 1 we show a sequence of images taken when the cork had a low density. Thanks to the relatively large speed of the process—it lasted approximately 3 h—it was possible to follow the rise until the cork reached the water surface. Both the marked point and the reference system used with Tracker are shown. In figure 6 the corresponding plot of the position of the cork versus time is shown. In the beginning, shots were taken every 5 min but, due to the high rise speed, the time intervals were soon reduced to 1 min. The trend shown in figure 6 exhibits the same features observed in all cases, also when the cork density was increased. There is an initial latency time during which the cork starts to randomly slip at the bottom of the jug, then the rise starts and the height increases almost linearly in time. What is extremely different

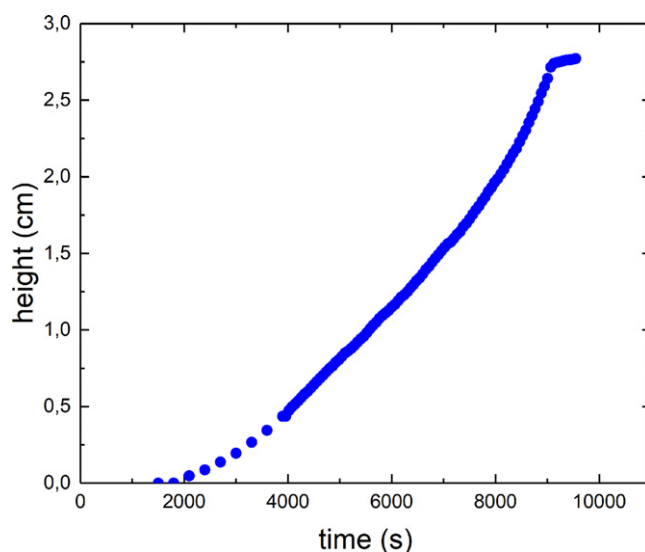


Figure 6. Cork's rise obtained by tracking the position of the marked point shown in figure 1.

from one measurement to another, and not easily predictable, are the typical latency times, which do not seem to depend trivially on the salt amount poured in water. There are probably multiple reasons for this behaviour. One is that the cork's density can slightly vary from one measurement to the other.

It is also very difficult to guarantee that the salt fills uniformly the bottom of the jug. Moreover, the finite size of the cork is not negligible with respect to the size of the jug. Therefore, the presence of the cork itself perturbs salt dissolution and therefore the typical times of the process. Finally, the temperature of the water is not controlled at all, therefore a change in the transport properties of the mixture is to be expected from one measurement to the other.

It is interesting to focus on the energy balance of the system in order to understand the relationship between the different mechanisms acting on the fluid and the cork. If one writes down the total mechanical energy of the cork as the sum of its gravitational potential energy plus its kinetic energy, when the cork is lifted from the bottom of the jug, the conservation of mechanical energy is obviously not satisfied, since the cork potential energy increases without any reason. In order to solve this apparent energy mystery, one should seek the origin of the force lifting the cork. The cork is subjected to the weight force, which is constant in time, and to the buoyancy determined by the surrounding liquid, which changes in time. The work needed to raise the cork is provided by the gradual increase of the density of the liquid surrounding the cork, determined by the diffusive dissolution of the salt. Therefore, the cork rises because the centre of mass of the fluid surrounding it gradually shifts upwards. This leaves us with another open question: what is the origin of the mechanical energy needed to lift the centre of mass of the fluid? The dissolution of salt provides an energy contribution to the system in terms of enthalpy and is driven by the thermal agitation of the component molecules $k_B T$. The energy is, in the end, taken from the thermal energy of the system, so that an accurate measurement of the fluid temperature should reveal a decrease of the temperature during the rise of the salt and the cork. This would, of course, be possible only in an ideal adiabatic system not exchanging

energy with other systems. In the experiment described here, the jug and the water are actually in thermal equilibrium with the surrounding environment, and the temperature increase is then not measurable since the environment acts as the ultimate thermal reservoir. Nevertheless, it is interesting to observe that in the initial condition, with the salt and the cork at the bottom of the jug, the potential energy of the system is at a minimum, while after some time, both the salt and the cork have been lifted increasing their potential energy at the expense of the enthalpy of the salt solution and ultimately to thermal energy. This is one of the cases of conversion of thermal energy to mechanical energy.

At any time during its rise, the cork floats in a stratified medium and, if set in vertical motion with a slight tap, it starts to oscillate at the Brunt–Väisälä frequency that is directly related to the local density gradient and gravity as shown in equation (10).

In figure 2, we show a sequence of shots of the cork that oscillates after a slight tap, given when it had reached approximately half height within the liquid. At a visual inspection, it was evident that the regular oscillations of the cork were periodically slowed down until the cork almost stopped, to start again to oscillate after a while. A video is included as supplemental material (video 1). In figure 7 we show a sequence of tracking of the oscillations taken at different times during the cork rise for a slow process where we used the cork with its final density. The periodical regular slowing down of the cork that can be observed in almost all the figures follows a complex dynamics, which cannot be trivially related to that of a damped harmonic oscillator. However, by fitting the first oscillations with the formula for a damped harmonic oscillator

$$y(t) = A * \cos(\omega * t) * \exp(-t/\tau) + y_0 \quad (30)$$

one gets a typical oscillation frequency ω in the range from 2.67 to 3.45 rad s⁻¹ and a damping constant τ from 2.38 to 4.87. The values of the frequency resulting from this simple fit are reported in figure 12.

A more accurate scrutiny of figure 7 reveals that the dynamics of the oscillations is similar to that observed for a beating phenomenon that occurs when two waves of slightly different frequencies interfere. As discussed at the end of section 4.3, the oscillations due to the gradient of density are expected to damp emitting transverse internal gravity waves that propagate perpendicularly to the direction of oscillation. Due to the finite size of the container, we expect that these waves are reflected back by the jug walls and finally interfere with the cork oscillation.

To test this hypothesis we performed a further experiment using a rectangular plexiglass tank as a container. We prepared another cork similar to the first one and immersed both of them in water and salt. As soon as the corks had reached a proper height, we slightly pushed one of them and verified that after a while also the other one started to oscillate. This is a piece of evidence that a signal propagated horizontally from the first cork to the second, as expected for internal gravity waves. In figure 3 an image of the two corks is shown, while a video is included as supplemental material (video 2). Gravity waves in a transparent fluid are almost invisible, and this feature makes them hard to investigate, but some of their features can be determined from their effect on bodies immersed in the fluid, such as the two corks that we used. A remarkable example is represented by the velocity of the wave, which can be obtained from the ratio $\frac{d_c}{t_m} = v = 6.6 \pm 1.4 \text{ cm s}^{-1}$, where $d_c = 8.3 \pm 0.5 \text{ cm}$ is the distance between the two corks, measured from the images, and $t_m \simeq 1.25 \pm 0.2 \text{ s}$ is the time interval between the push on the first cork and the time at which the second one starts to oscillate itself. A more thorough investigation of the process requires the possibility of visualizing the wave. This is made possible by the fact that the waves occur through density variations, which are associated with changes in the index of refraction. These perturbations can be effectively detected using interferometric optical techniques, such as Schlieren, which allow mapping the modulations

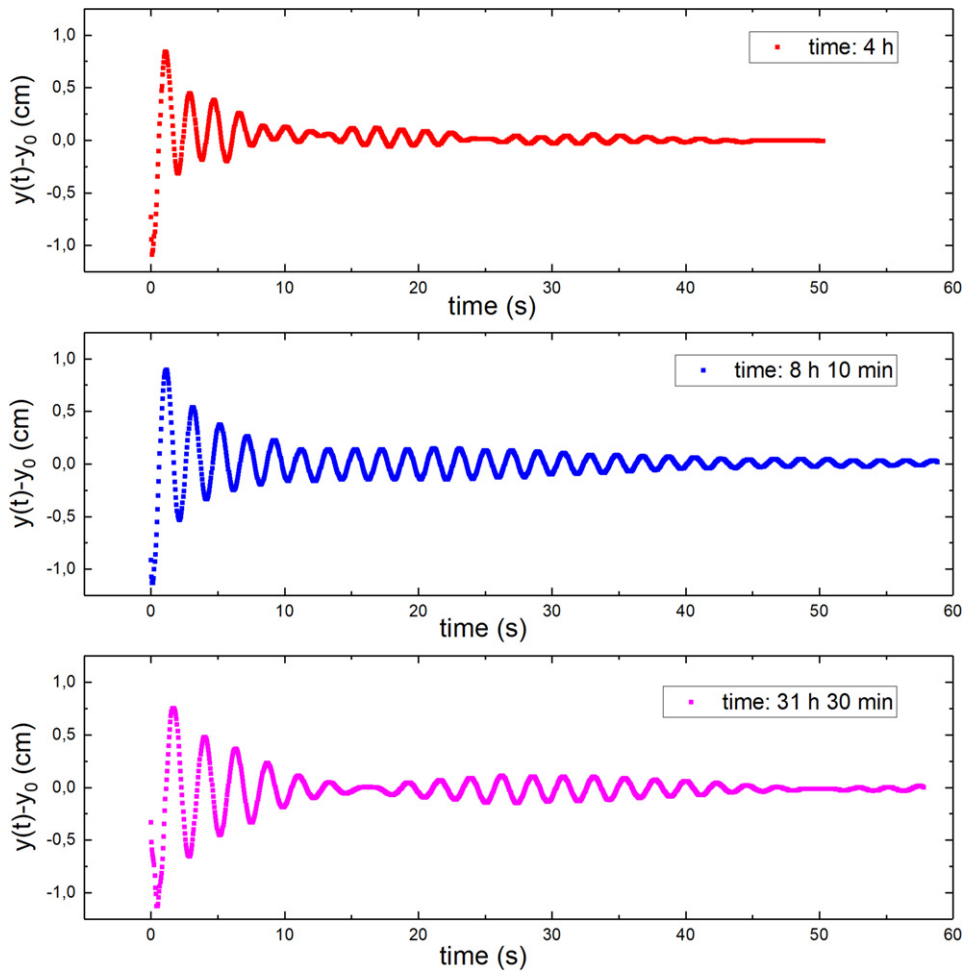


Figure 7. Tracking of the cork oscillation taken at different times of the same measurement with 30 g l^{-1} NaCl.

of the index of refraction as intensity variations. In this paper, however, we chose a different approach, easier to be used even far from a laboratory. We visualize them by observing the deformations of a reference object placed behind the liquid. In this experiment, we used a chequered sheet placed in contact with the back window of the tank. To analyse the gravity waves, we processed the images of the two corks with Fiji by expanding the images in the vertical direction by a factor of 16 to achieve better visualization of the horizontal lines of the chequered reference pattern. Images were then converted to grayscale and a gamma correction of exponent 3 was applied to increase the contrast of the horizontal lines. A video is available as supplemental material (video 3). In figure 8 we show a sequence of processed images collected at different times after the start of oscillations of the first cork. The deformation of the horizontal line can be clearly observed and used to calculate the speed and frequency of the internal gravity wave. The positions of the wave peaks were followed in time with the Tracker programme, and in figure 9, a plot of the displacement along the x -direction vs time for one of them is shown.

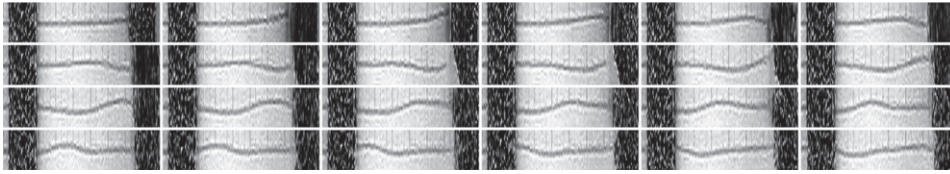


Figure 8. Sequence of images taken with a frame rate of 8 img s^{-1} at different times of a portion of the sheet of paper placed behind the tank between the two corks. Time increases from left to right and from top to bottom. The horizontal line is deformed due to the variation of the refractive index produced by the transit of the internal gravity wave. A video is available as supplemental material (video 3).

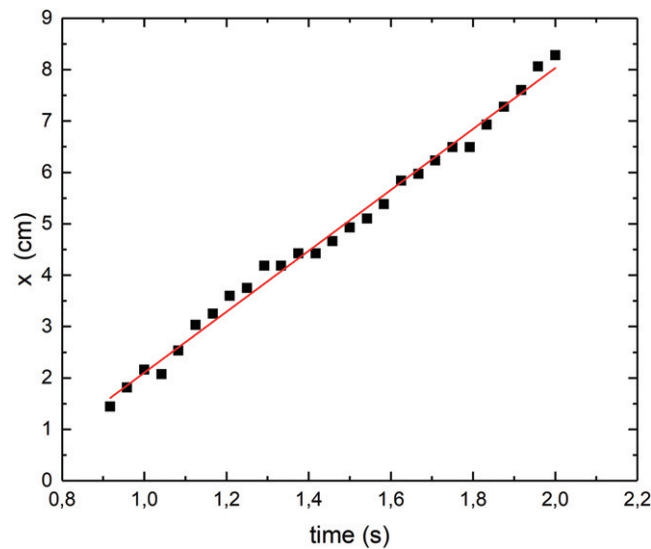


Figure 9. Peak position of the wave detectable as a deformation of the line shown in figure 8. The solid line is the best linear fit of the experimental points and its slope gives an estimate of the wave speed that, for this curve is $6.0 \pm 0.1 \text{ cm s}^{-1}$.

The continuous straight line is the best linear fit of the experimental points and its slope gives an estimate of the wave speed $v_w \approx 6.0 \pm 0.1 \text{ cm s}^{-1}$.

We have tracked three different peaks spanning the space between the two corks obtaining an average value for v_w , $v_{av} = 6.7 \pm 0.6 \text{ cm s}^{-1}$.

We also measured the frequency of the internal gravity wave by using the line deformations along the vertical direction, induced by the index of refraction inhomogeneities shown in figure 8. Using the Tracker programme, fixed points of the line were chosen and followed in time during the passage of the wave to measure their displacement along the y -axis. A typical result is shown in figure 10.

The continuous line is the best fit of the experimental points with equation (30). By averaging the oscillation frequencies obtained by tracking different points of the line, we obtained an average value for $\omega = 4.4 \pm 0.4 \text{ rad s}^{-1}$ that corresponds to a frequency $f = 0.64 \pm 0.06 \text{ Hz}$ for the internal gravity wave. This value is close to the oscillation frequency of the cork pushed

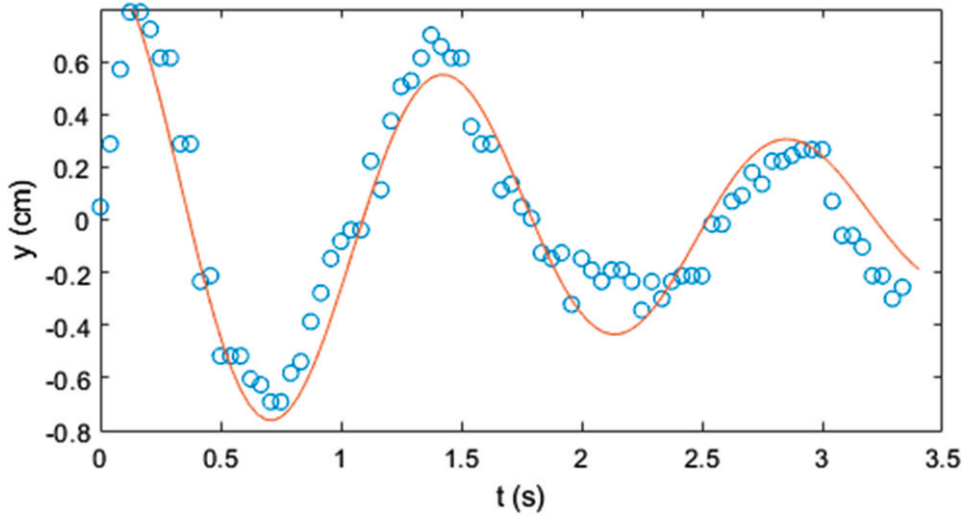


Figure 10. Tracking of the position of a point on the line shown in figure 8 during the passage of the gravitational wave. The continuous line is the fit obtained using equation (30).

in motion, $\omega_c = 4.26 \text{ rad s}^{-1}$, as measured by tracking the cork position. This result confirms that the internal gravity wave has the same frequency as the Brunt–Väisälä wave that generates it, as shown in equation (29), although it must be stressed that the image quality and the strong damping of the waves make it difficult to obtain a precise estimation of the frequencies.

To have better quality measurements of Brunt–Väisälä frequencies in different conditions, we finally fitted the individual cork's oscillations shown in figures 2 and 7. In order to fit the entire curves and not only the first oscillations, we used a phenomenological fitting function more refined with respect to equation (30) that takes into account both the oscillation damping and the beatings between the cork oscillation and the back-reflected internal gravity wave:

$$y(t) = A * \cos(\omega_1 * t + \phi_1) * \cos(\Delta\omega * t + \phi_2) * \exp(-(t/\tau)^\gamma) + y_0, \quad (31)$$

where ω_1 , $\Delta\omega$, ϕ_1 , ϕ_2 , τ , γ and y_0 are the free parameters. Equation (31) is the product of two cosine functions which typically describes beatings that occur when two waves of similar frequencies interfere. In beating phenomena, ω_1 is the average of the frequencies of the interfering waves, while $\Delta\omega$ is their difference. A tentative explanation of the slightly different frequencies between the cork and the reflected wave, could be that the viscous dissipation damps the oscillations of the cork and the wave differently. It is known that damping of the oscillations reduces their frequencies, therefore the frequencies of the cork and that of the wave will be slightly different and both smaller than the Brunt–Väisälä one. The stretched exponential term $\exp(-(t/\tau)^\gamma)$ with $\gamma = 2$ turned out to be the best function to account for the severe damping of the two oscillating terms that have different time constants. In figure 11 we show the remarkable result of the fit. It can be noticed that while equation (30) is able to fit only the first oscillations, equation (31) is able to account for all the oscillations features.

As shown in figure 12, for all the data shown in figure 7, $\Delta\omega$ is much smaller than ω_1 and this result confirms that the two beating waves have very close frequencies.

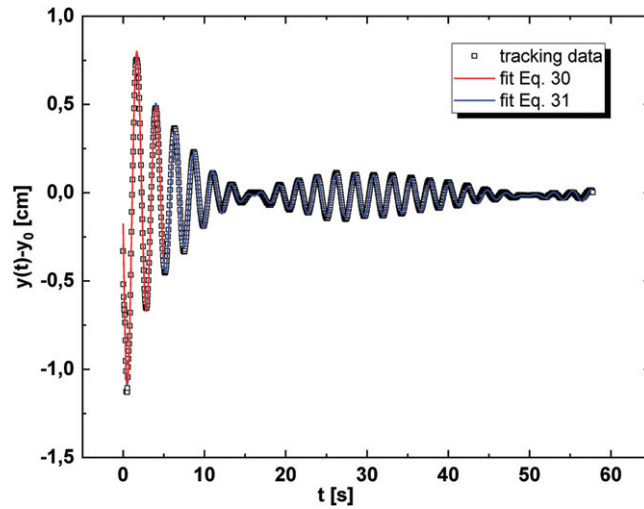


Figure 11. Fit of the oscillation tracking for a measurement performed with 30 g l^{-1} NaCl. Data are taken 4 h after the beginning of data acquisition, when the cork was almost 1.5 cm from the bottom of the jug.

As a consequence, ω_1 gives a good estimation of the Brunt–Väisälä frequency and turns out to be in very good agreement with the frequency ω that is obtained by fitting the data with the much simpler equation (30). In figure 12, it can be appreciated that the frequency of oscillation decreases in time as expected because the density gradient diminishes while the concentration approaches the final equilibrium value.

From the Brunt–Väisälä frequency, it is possible to calculate the value of the density gradient $\frac{\partial \rho}{\partial z}$ from equation (10). Having fitted all the oscillations measured with all the different salt concentrations, we found for the frequency $N = \omega$ values between 1,5 and 4,5 rad s^{-1} depending on the initial salt concentration and the height of the cork in the fluid and on the time of the measurement. Using equation (10) the corresponding values for $\frac{\partial \rho}{\partial z}$ ranges from 236 kg m^{-4} to 2140 kg m^{-4} corresponding to concentration variations $\frac{\partial c}{\partial z} = \frac{\partial \rho}{\partial z} / \frac{\partial \rho}{\partial c}$ ranging from 0.32 m^{-1} to 3.0 m^{-1} , where for a solution of NaCl in water at small concentration $\frac{\partial \rho}{\partial c} = 720 \text{ kg m}^{-4}$ [28].

Finally, we remark that in the case discussed in our experiment, the motion of the cork generates a wave that propagates radially in the horizontal direction due to the fact that the system is circularly symmetric with respect to the direction of the oscillation that is parallel to the density gradient. In more general terms, gravity waves can be obtained by forcing, in an arbitrary direction, the oscillations of a body immersed into the fluid [22, 29], leading to a phenomenology much richer than the one discussed in this paper. Mowbray and Rarity [29] performed refined experiments in the presence of a constant density gradient, leading to accurate experimental results. In their experiments the oscillations are imposed in a nearly horizontal direction and the response of the system is investigated as a function of the external forcing frequency. As the density gradient is vertical, imposing a horizontal oscillation, breaks the symmetry of the system leading to the formation of more complex wave patterns.

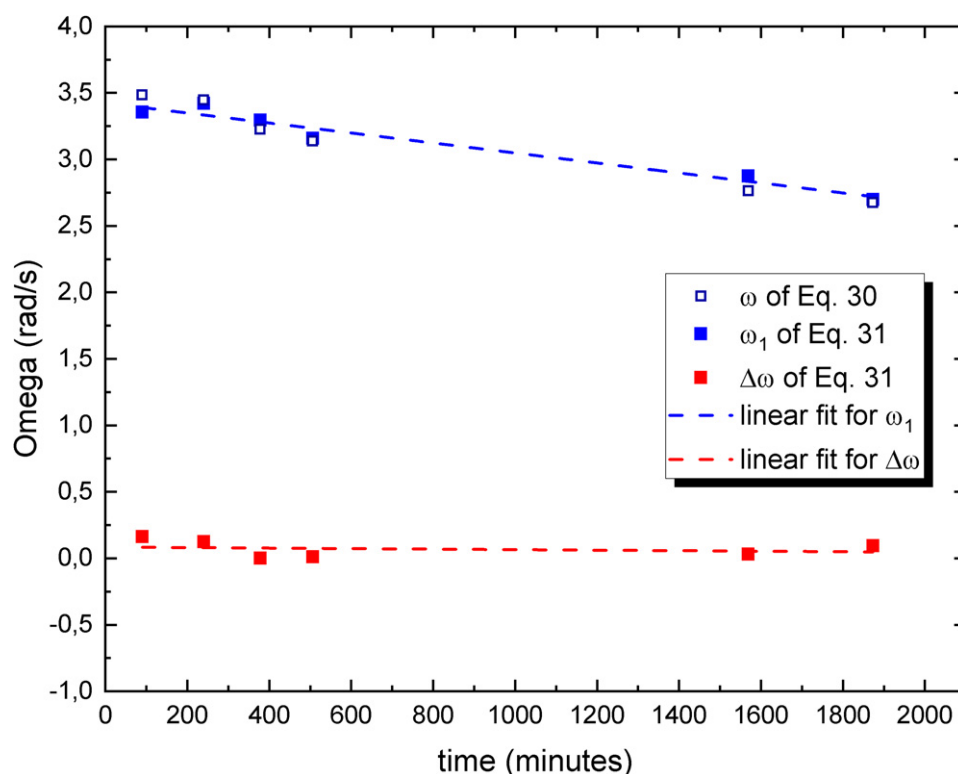


Figure 12. The plot shows the values of ω_1 (blue squares) and $\Delta\omega$ (red squares), as obtained by fitting the data in figure 7 with equation (31). Open squares are the values of ω obtained by fitting the first oscillations of the same data with equation (30). Both ω and ω_1 give a good estimation of the Brunt–Väisälä frequency.

6. Conclusions

We have discussed an engaging, inexpensive, and simple experiment that allows introducing undergraduate students to many arguments on hydrostatic, buoyancy, and levitation in a stratified fluid. The general scientific framework of levitation, and the theoretical description of the phenomena that are experimentally accessible, are also presented in this work. Brunt–Väisälä oscillations are observed and the measurement of their frequency may be used to estimate the concentration gradient inside the fluid. Moreover, the effect of gravity waves can be observed and measured. We propose a phenomenological function to fit the data, able to keep into account both the damping of the oscillations and the beatings with the internal gravity wave they generate. The motion of the cork determines a partial remixing of the stratified fluid, thus reducing the concentration gradient that drives the oscillations. In this respect, the experiment represents a remarkable example of a classical system where performing a measurement significantly affects the state of the system. This feature makes a long series of repeated measurements not useful, in contrast with the usual physical systems usually encountered by students during laboratory activities. The experiment is exploitable by students of any age as the level of deepening can be tuned as a function of the students' knowledge. However, it is particularly suitable for undergraduate students that can appreciate all its implications.

Acknowledgments

Work partially supported by the European Space Agency, CORA-MAP TechNES Contract No. 4000128933/19/NL/PG. This research was carried under the framework of the E2S UPPA Hub Newpores and Industrial Chair CO2ES supported by the ‘Investissements d’Avenir’ French programme managed by ANR (ANR–16–IDEX–0002).

ORCID iDs

Marina Carpineti  <https://orcid.org/0000-0002-8766-703X>

Fabrizio Croccolo  <https://orcid.org/0000-0001-6832-400X>

Alberto Vailati  <https://orcid.org/0000-0002-3119-6021>

References

- [1] Brandt E H 1989 *Science* **243** 349
- [2] Callens N, Ventura-Traveset J, de Lophem T-L, Lopez de Echazarreta C, Pletser V and van Loon J J W A 2011 *Microgravity Sci. Technol.* **23** 181–9
- [3] Sorokin V and Blekhman I I 2020 *Nature* **585** 31–2
- [4] Apffel B, Novkoski F, Eddi A and Fort E 2020 *Nature* **585** 48–52
- [5] Braibanti M et al 2019 *Eur. Phys. J. E* **42** 86
- [6] Jones T B, Washizu M and Gans R 1997 *J. Appl. Phys.* **82** 883
- [7] Nappo C J 2012 *An Introduction to Atmospheric Gravity Waves* (Amsterdam: Elsevier)
- [8] Le Bars M D L 2020 *Fluid Mechanics of Planets and Stars* (Berlin: Springer)
- [9] Millikan R A 1913 *Phys. Rev.* **2** 109
- [10] Millikan R A 2021 Nobel lecture <https://nobelprize.org/prizes/physics/1923/millikan/lecture/> (accessed 26 January 2021)
- [11] Landau L D and Lifshitz E M 1960 *Electrodynamics of Continuous Media* (Oxford: Pergamon)
- [12] Saslow W M 1991 *Am. J. Phys.* **59** 16
- [13] Powell J R and Danby G T 1971 *Cryogenics* **11** 192
- [14] Coffey H T 1994 Status of maglev: opportunities in cryogenics and superconductivity *Advances in Cryogenic Engineering* vol 39, ed P Kittel (Boston, MA: Springer)
- [15] Berry M V and Geim A K 1997 *Eur. J. Phys.* **18** 307
- [16] Marzo A, Barnes A and Drinkwater B W 2017 *Rev. Sci. Instrum.* **88** 085105
- [17] Ashkin A 1970 *Phys. Rev. Lett.* **24** 156
- [18] Ashkin A 2021 Nobel lecture <https://nobelprize.org/prizes/physics/2018/ashkin/lecture/> (accessed 25 January 2021)
- [19] Moffitt J R, Chemla Y R, Smith S B and Bustamante C 2008 *Annu. Rev. Biochem.* **77** 205
- [20] McGloin D and Reid J P 2010 *Opt. Photonics News* **21** 20
- [21] Vogel S 2013 *Comparative Biomechanics* (Princeton, NJ: Princeton University Press)
- [22] Lighthill M J 1967 *Commun. Pure Appl. Math.* **20** 267
- [23] Croccolo F, García-Fernández L, Bataller H, Vailati A and Ortiz de Zárate J M 2019 *Phys. Rev. E* **99** 012602
- [24] Douglas B, Wolfgang C and Robert M H 2021 Tracker - video analysis and modeling tool <https://physlets.org/tracker/> (accessed 29 12 2020)
- [25] Schindelin J, Arganda-Carreras I, Frise E, Kaynig V, Longair M, Pietzsch T and Cardona A 2012 Fiji: an open-source platform for biological-image analysis *Nat. Methods* **9** 676–82
- [26] Segré E 1970 *Enrico Fermi Physicist* (Chicago, IL: University of Chicago Press)
- [27] Tritton D J 1988 *Physical Fluid Dynamics* (Oxford: Clarendon)
- [28] Lide D R 2005 *CRC Handbook of Chemistry and Physics* 86th edn
- [29] Mowbray D E and Rarity B S H 1967 *J. Fluid Mech.* **28** 1